

Stochastic Nonparametric Estimation of the Fundamental Diagram

Iaroslav Kriuchkov^{a,*}, Timo Kuosmanen^b

^a*Aalto University School of Business, 02150 Espoo, Finland*

^b*Turku School of Economics, University of Turku, 20500 Turku, Finland*

May 2023

Abstract

The fundamental diagram serves as the foundation of traffic flow modeling for almost a century. With the increasing availability of road sensor data, deterministic parametric models have proved inadequate in describing the variability of real-world data, especially in congested area of the density-flow diagram. In this paper we estimate the stochastic density-flow relation introducing a nonparametric method called *convex quantile regression*. The proposed method does not depend on any prior functional form assumptions, but thanks to the concavity constraints, the estimated function satisfies the theoretical properties of the fundamental diagram. The second contribution is to develop the new *convex quantile regression with bags* (CQRb) approach to facilitate practical implementation of CQR to the real-world data. We illustrate the CQRb estimation process using the road sensor data from Finland in years 2016-2018. Our third contribution is to demonstrate the excellent out-of-sample predictive power of the proposed CQRb method in comparison to the standard parametric deterministic approach.

Keywords: convex regression, quantile regression, density-flow diagram, traffic flow theory, sensor data

*Corresponding author

Email addresses: iaroslav.kriuchkov@aalto.fi (Iaroslav Kriuchkov), timo.kuosmanen@utu.fi (Timo Kuosmanen)

1. Introduction

Traffic congestion arises when the demand for the road space exceeds the available capacity. Congestion has numerous detrimental effects such as delays, increased fuel consumption, air pollution, vehicle wear and tear, and higher collision risks (Figliozzi, 2011; Bigazzi & Figliozzi, 2013). Recognizing the negative consequences of congestion, researchers and policymakers have been exploring effective methods for managing traffic flow to alleviate congestion. One promising avenue that holds substantial potential lies in leveraging road sensor data, which provides valuable real-time insights into traffic conditions and patterns (Guériau et al., 2016; Shaygan et al., 2022).

Within the realm of the traffic flow theory, the fundamental diagram plays a pivotal role in understanding the relationship between traffic flow, density, and speed. Originating from the seminal work of Greenshields et al. (1935) this concept has been extensively studied and applied in transportation research. Traditionally, the density-flow relation is modeled using simple parametric functional forms specifications such as piece-wise linear triangular (bi-linear) forms (Newell, 1993), truncated piece-wise linear triangular (bi-linear) forms (Daganzo, 1994), or quadratic-linear forms (Smulders, 1990). Note that all these classic formulations assume a concave relation between the density and flow.

In empirical research, deterministic approaches remain widely used for estimating the fundamental diagram from observed road sensor data (Lighthill & Whitham, 1955; Zhang, 1999; Wang et al., 2011; Coifman, 2014). However, these models are unable to predict the variance in the free-flow part of the fundamental diagram, let alone the congested part (Zhang, 1999). Empirical road sensor data shows that such deterministic characterizations are far from reality due to the heterogeneity in types of vehicles, driver behavior, and the use of advanced driver-assistance systems (ADAS). To account for random heterogeneity in data, stochastic fundamental diagrams have started to gain popularity in the recent empirical literature (Hoogendoorn & Bovy, 1998; Jabari & Liu, 2012; Qu et al., 2017).¹ Various

¹Other attempts to describe heterogeneity include the models that allow for the capacity drop (Edie, 1961; Cassidy & Bertini, 1999), three-phase approach (Kerner & Konhäuser, 1994; Kerner, 2009) and accounting for differences between types of vehicles and drivers (Chanut & Buisson, 2003).

approaches have been proposed to incorporate stochasticity into the fundamental diagram modeling. One such approach involves adding noise to deterministic relations, as demonstrated in works by Muralidharan et al. (2011) and Wang et al. (2013). Data-driven relation has gained momentum since then with numerous studies being conducted by Fan & Seibold (2013); Qu et al. (2017) and Wang et al. (2021). Despite these advances, it is important to note that these methods are still predominantly parametric, which means that they require a specified functional form (Bramich et al., 2022).

This paper proposes a fully nonparametric approach to estimating the stochastic fundamental diagram on the density-flow plane.² Our method builds upon and extends the *convex quantile regression* (CQR) approach by Wang et al. (2014); Kuosmanen et al. (2015) and Dai et al. (2022), which belongs to the family of the convex regression models and related nonparametric estimators subject to convexity (concavity) constraints. To our knowledge, this study presents the first application of the convex regression approach to estimating the fundamental diagram from empirical data. The proposed approach fits a piece-wise linear function without any prior restrictions on the number of pieces or their location. We do not need to assume piece-wise linear functional form *a priori*, rather, the piece-wise linear functional form has been shown capable to represent any arbitrary concave function (Kuosmanen, 2008).³ The proposed method satisfies all the theoretical properties of the fundamental diagram noted by del Castillo (2012). Quantiles have been independently used in the context of estimation the speed-flow relation by Wang et al. (2021) however, they rely on the parametric specifications of the functional form whereas our approach is fully nonparametric.

Since the density-flow relation is fundamentally concave, we would argue that the convex regression and CQR provide useful tools for the estimation in the stochastic setting with

²The term nonparametric does not necessarily imply the absence of assumptions, and it is not necessarily the case that the assumptions of a nonparametric model are less restrictive than those of a parametric model. Following Chen (2007), an econometric model is termed “nonparametric” if all of its parameters are in infinite-dimensional parameter spaces.

³The term convex regression refers to the fact that the support function of a convex set is globally concave or convex. Therefore, convex regression can be used for estimating globally concave or convex functions.

heterogeneous vehicle data. The concavity property was first recognized by Ansorge (1990), fully formulated by Castillo & Benitez (1995) with its role explained within the variational theory of traffic flow by Daganzo (2005). Although the concavity of the fundamental diagram in the density-flow plane has also attracted some critical debate (Koshi et al., 1983; Hall & Agyemang-Duah, 1991), we note that the solutions with deceleration shockwaves for the Lighthill–Whitham–Richards model (Lighthill & Whitham, 1955; Richards, 1956) can only be obtained in the concave case.

Our second contribution is to develop the new *convex quantile regression with bags* (CQRb) method to facilitate practical implementation of CQR to the real-world road sensor data. We illustrate the estimation process and the obtained function using the proposed method. The example is provided with the use of road sensor data from Finland (see Section 5 for details).

The third contribution is the first out-of-sample performance evaluation of the proposed method on the real-world road sensor data. Applying insights from the machine learning literature, we partition the observed sample to a training set and a test set to objectively assess the predictive power of the proposed method. In addition, we compare the performance of our method with the renowned method for the estimation of fundamental traffic flow parameters for triangular fundamental diagram introduced by Dervisoglu et al. (2009) (hereinafter DGKHV).

The rest of the paper is organized as follows. In Section 2 we discuss the estimation of the fundamental diagram on the density-flow plane and introduce the idea of shape-constrained least-squares regression in additive formulation, further extending it to the nonparametric formulation with the introduction of quadratic programming problem. We further show how the aforementioned model is transformed into convex quantile regression with linear programming formulations in Section 3. After that we discuss the computational aspects of the estimations introducing bagging and the related convex quantile regression with bags (CQRb) in section 4. We provide an illustrative application example to Finnish road sensor data in Section 5 and evaluate the performance of the proposed method in Section 6. Section 7 concludes.

2. Preliminaries on the traffic flow theory and convex regression

2.1. Fundamental diagram

The fundamental diagram of traffic flow represents the relation between three variables: traffic flow (q), traffic speed (v) and traffic density (k). The diagram can be projected onto three main planes: to density-flow plane $q = f(k)$, to density-speed plane and to speed-flow plane. These projections are interconnected through the fundamental relation proposed by Lighthill & Whitham (1955):

$$q = kv \tag{1}$$

There are two primary approaches to fundamental diagram estimation: through density-flow relation (Smulders, 1990; Newell, 1993; Daganzo, 1994) and through density-speed relation (Wu, 2002; Qu et al., 2015, 2017). While both have been extensively studied in the literature, our focus is on the estimation of density-flow relation $q = f(k)$, as the method we propose is inherently concave as discussed in the Introduction. Moreover, it is widely accepted that increasing interaction between vehicles, meaning higher density, is the cause of the variance in traffic speed and traffic flow (Hernandez et al., 2002; Tadaki et al., 2015).

In this method, we focus on concave shapes of density-flow relations of the fundamental diagram, as these forms are the predominant in the traffic flow research with concavity property playing an important role in the literature (Ansorge, 1990; Castillo & Benitez, 1995; Daganzo, 2005). It is worth mentioning that the concave shape of the fundamental diagram in density-flow plane is also recognized to be useful for traffic management purposes (Keyvan-Ekbatani et al., 2012; Roncoli et al., 2016). The peak flow rate (q_c) and the corresponding density (k_c), as well as the jam density (k_j) can be easily derived from the concave fundamental diagram. This way the strategies can be developed to minimize congestion and to prevent the actual density from exceeding the critical density ($k > k_c$).

In the stochastic setting, the density-flow relation can be stated as a regression equation:⁴

$$q_i = f(\mathbf{k}_i) + \varepsilon_i \quad \forall i, i = 1, \dots, n \tag{2}$$

⁴For clarity, we denote vectors with bold lowercase symbols (e.g. \mathbf{k}). All vectors are column vectors. As the focus of this paper is density-flow relation, the standard notation of k for density and q for flow is used.

where $\mathbf{k}_i = (k_{i1}, k_{i2}, k_{i3}, \dots, k_{im})^\top$ represents a m -dimensional vector $\mathbf{k} \in \mathbb{R}^m$ of predictors, including traffic flow k (potentially observed on multiple lanes), and q_i is a response variable for some observation i . The error term ε has a zero mean $E(\varepsilon_i) = 0 \quad \forall i$ and finite variance $V(\varepsilon_i) < \infty \quad \forall i$. In the context of road traffic the error grasps the fluctuations in road conditions, for example weather and traffic composition.

2.2. Convex regression

Suppose the regression function $f : \mathbb{R}^m \rightarrow \mathbb{R}$ is unknown but satisfies certain shape restrictions, such as concavity, monotonicity, and homogeneity (see Kuosmanen & Johnson (2010) and Yagi et al. (2020) for a more detailed discussion).

Hildreth (1954) is the pioneer in the study of nonparametric regression with monotonicity and concavity constraints in the case of a single explanatory variable k . Kuosmanen (2008) further develops Hildreth's approach by extending it to the case of a vector-valued \mathbf{k} in a multivariate setting, and refers to this method as *convex nonparametric least squares* (CNLS). In this CNLS method, it is assumed that the function f belongs to a set of continuous, monotonically increasing, and globally concave functions called F_2 , and $\mathcal{F} \subset F_2$. For the specifics of the fundamental diagram application, we will focus only on the set of concave functions $\mathcal{F} = \{f : \mathbb{R}_+^m \rightarrow \mathbb{R}_+ \mid \forall \mathbf{k}_1, \mathbf{k}_2 \in \mathbb{R}_+^m : \mathbf{k}_1 < \mathbf{k}_2, f((1-\alpha)\mathbf{k}_1 + \alpha\mathbf{k}_2) \geq (1-\alpha)f(\mathbf{k}_1) + \alpha f(\mathbf{k}_2)\}$, which contains the regression function f . The CNLS estimator of function f is defined as the optimal solution to the following infinite dimensional least squares problem:

$$\begin{aligned} \min_{\alpha, \beta, \varepsilon} \quad & \sum_{i=1}^n \varepsilon_i^2 \\ \text{s.t.} \quad & q_i = \alpha_i + \boldsymbol{\beta}_i^\top \mathbf{k}_i + \varepsilon_i \quad \forall i \\ & f \in F_2 \end{aligned} \tag{3}$$

It is important to note that the functional form of f is not predetermined. However, F_2 consists of infinite number of functions. As a result, this problem cannot be solved using a simple trial-and-error approach. The main challenge is to introduce the convexity (concavity) constraint, as there is no determined functional form.

In the multivariate case (\mathbf{k}_i, q_i) , $i = 1, \dots, n$, the following finite dimensional quadratic programming problem Kuosmanen (2008) should be solved:

$$\begin{aligned}
& \min_{\alpha, \beta, \varepsilon} \sum_{i=1}^n \varepsilon_i^2 \\
& \text{s.t.} \quad q_i = \alpha_i + \beta_i^\top \mathbf{k}_i + \varepsilon_i \quad \forall i \\
& \quad \alpha_i + \beta_i^\top \mathbf{k}_i \leq \alpha_s + \beta_s^\top \mathbf{k}_i \quad \forall i, s \quad i \neq s
\end{aligned} \tag{4}$$

In problem (4), the objective function minimizes the sum of squared errors. Coefficients α_i and β_i are the intercept and slope coefficients of the tangent hyperplanes that describe the estimated piece-wise linear function \hat{f} . The multiplication $\beta_i^\top \mathbf{k}_i$ is a vector product of a transposed vector of slope coefficients β_i and a vector of explanatory variables \mathbf{k}_i ($\beta_i^\top \mathbf{k}_i = \beta_{i1}k_{i1} + \beta_{i2}k_{i2} + \dots + \beta_{im}k_{im}$). The first constraint of the problem expresses the regression equation (2) in terms of a piece-wise linear approximation of the true, yet unknown, regression function f . The second constraint requires the concavity of the estimated function (to impose convexity, the inequality sign should be reversed). In Kuosmanen (2008) the monotonicity assumption is imposed by adding the constraint $\beta_i \geq \mathbf{0} \quad \forall i$, but in the present context we relax it.

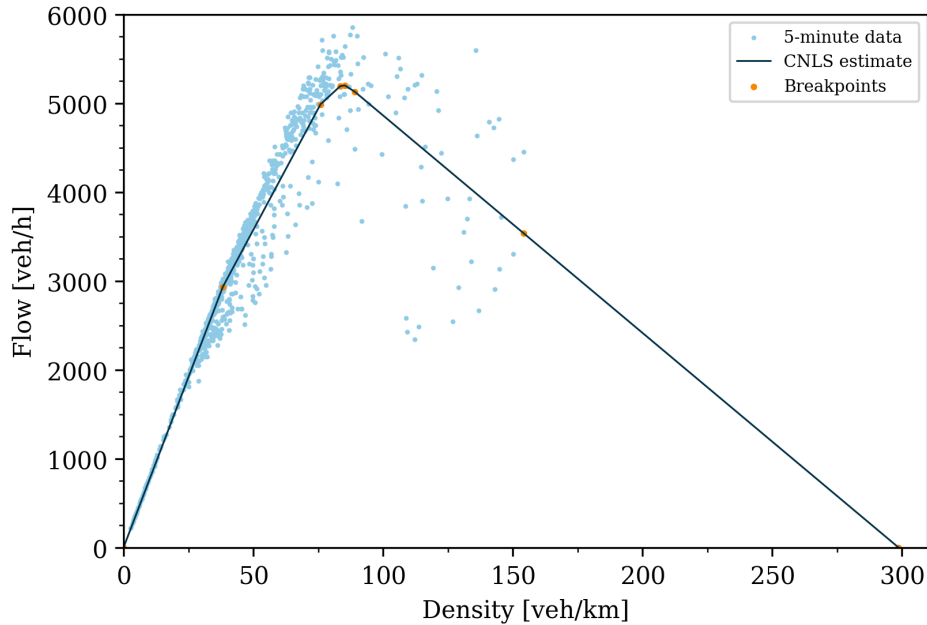


Figure 1: Illustration of the fitted function estimated with CNLS

The solution of problem (4) yields a unique pair of slope and intercept coefficients $(\hat{\alpha}_i, \hat{\beta}_i)$ for each observation i , resulting in the best possible fit. The piece-wise linear function f is constructed using these pairs $(\hat{\alpha}_i, \hat{\beta}_i)$, meaning $\hat{f}_i = \hat{\alpha}_i + \hat{\beta}_i \mathbf{k}_i$. In practice, the number of segments of a piece-wise linear function is considerably smaller than the number of observations. In the estimation of density-flow relation the meaning of β_i is the shockwave speed except for β_1 , which denotes the vehicle speed, which is equal to the shockwave speed in the first piece.

Figure 1 illustrates the example of the CNLS estimation on 5-minute-data from a traffic measurement station (see Section 5 for a detailed description of the data). Breakpoints on the figure illustrate the connections between different pieces. Note that the shockwave speed gradually decreases as density k increases. At the critical density of $k = 85.29$, the sign of the shockwave speed becomes negative, as illustrated by the downwards sloping part of the density-flow diagram in Figure 1. The estimated piece-wise linear function depicted in Figure 1 can be explicitly stated as follows.

$$\hat{f}(k) = \begin{cases} 76.88k + 45.12 & 0 \leq k \leq 38.29 \\ 55.48k + 864.03 & 38.29 \leq k \leq 75.93 \\ 15.37k + 3910.85 & 75.93 \leq k \leq 83.54 \\ 2.93k + 4951.16 & 83.54 \leq k \leq 85.29 \\ -16.91k + 6644.69 & 85.29 \leq k \leq 89.07 \\ -24.34k + 7306.55 & 89.07 \leq k \leq 300.19 \end{cases} \quad (5)$$

For a univariate case $m = 1$ of problem (4) the convexity constraint can be simplified following Hanson & Pledger (1976) and Lee et al. (2013) for more efficient computations. The simplification requires the sorting of the observed data in ascending order according to k . The simplified problem has the following formulation (6).

$$\begin{aligned} \min_{\alpha, \beta, \varepsilon} \quad & \sum_{i=1}^n \varepsilon_i^2 \\ \text{s.t.} \quad & q_i = \alpha_i + \beta_i k_i + \varepsilon_i \quad \forall i \\ & \beta_i \leq \beta_{i-1} \quad \forall i, i = 2, \dots, n \\ & \alpha_i \geq \alpha_{i-1} \quad \forall i, i = 2, \dots, n \end{aligned} \quad (6)$$

The concept of using a piece-wise linear function \hat{f} is applied in a different context to the estimation of the macroscopic fundamental diagram (MFD). Daganzo & Geroliminis (2008) propose an analytical approximation of the MFD using a technique referred to as “tight cuts”, which is similar in spirit to the CNLS method.

3. Convex quantile regression

Traffic data is known to be widely scattered (Treiber et al., 2006), and various explanations have been proposed for this phenomenon, including stochastic effects (Gipps, 1981) and the heterogeneity of traffic (Daganzo et al., 1999). The congested part of the fundamental diagram, which is plotted on the density-flow plane, has substantially higher variance compared to the uncongested part. Furthermore, estimating the conditional mean flow for a given density is not always a priority for traffic researchers, as it requires a deterministic capacity value and may bias the shockwave speed. To address these issues, we propose to use the quantile regression to estimate the density-flow relation of the fundamental diagram. Quantile regression, in one way or another, has been used to estimate the fundamental diagram in the works of Dervisoglu et al. (2009), Li & Zhang (2011) and Wang et al. (2021). We next expand the quantile regression to convex quantile regression (CQR), extending the CNLS approach.

Convex nonparametric least squares (CNLS) estimates the conditional mean $E(q_i|\mathbf{k}_i)$ of the response variable. Quantile regression serves as a generalization of classical mean regression model by estimating some conditional quantile $Q_q(\tau|\mathbf{k})$, $\tau \in (0, 1)$ (Koenker & Bassett, 1978; Koenker, 2005):

$$Q_q(\tau|\mathbf{k}) = F^{-1}(\tau|\mathbf{k}) = \inf\{q \geq 0 \mid F(q|\mathbf{k}) \geq \tau\} \quad (7)$$

where $F(q|\mathbf{k})$ is the conditional distribution function of q given $\mathbf{k} \leq \mathbf{k}$. If the observed \mathbf{k} are exogenous, then the quantile function can be equivalently stated (Dai et al., 2023) as

$$Q_q(\tau|\mathbf{k}_i) = f(\mathbf{k}_i) + F_{\varepsilon_i}^{-1}(\tau) \quad (8)$$

In the context of convex regression, the *convex quantile regression* (CQR) provides an analogous extension to CNLS. In practice, what differentiates CQR from CNLS is the loss

function. While CNLS uses the symmetric least squares as the objective function, CQR utilizes the asymmetric least absolute loss, also known as quantile loss function $\rho_\tau(\xi) = \xi(\tau - \mathbb{I}_{\xi < 0})$, where \mathbb{I}_A is an indicator function. Following Wang et al. (2014); Kuosmanen et al. (2015) and Dai et al. (2022) we extend the CNLS problem to estimate CQR in the following section.

3.1. Convex quantile regression (CQR) programming problem

Denoting a pre-specified quantile as $\tau \in (0, 1)$, the *convex quantile regression* (CQR) linear programming problem is formulated as:

$$\begin{aligned} \min_{\alpha, \beta, \varepsilon^+, \varepsilon^-} \quad & \tau \sum_{i=1}^n \varepsilon_i^+ + (1 - \tau) \sum_{i=1}^n \varepsilon_i^- \\ \text{s.t.} \quad & q_i = \alpha_i + \beta_i^\top \mathbf{k}_i + \varepsilon_i^+ - \varepsilon_i^- \quad \forall i \\ & \alpha_i + \beta_i^\top \mathbf{k}_i \leq \alpha_s + \beta_s^\top \mathbf{k}_i \quad \forall i, s, \quad i \neq s \\ & \varepsilon_i^+ \geq 0, \quad \varepsilon_i^- \geq 0 \quad \forall i \end{aligned} \tag{9}$$

Here the error term consists of two non-negative components $\varepsilon^+, \varepsilon^- \geq 0$, so the objective function minimizes the absolute deviations instead of the symmetric quadratic. The first three constraints of problem (9) are the same as those of the CNLS problem (4). The last constraint makes the components of additive error term non-negative. Using the same approach as for problem (6), it is possible to formulate a simplified approach for a univariate case $m = 1$.

The pre-specified quantile $\tau \in (0, 1)$ defines the quantile to be estimated. For example, by setting the $\tau = 0.9$, the piece-wise linear CQR function envelopes at most 90% of observations, and at most 10% of the observations lie above the fitted function. With $\tau = 0.5$ the conditional median is estimated.

One key difference between CNLS and CQR is that the objective function for CQR is linear. With all constraints being linear functions of unknown parameters, the CQR problem (9) can be solved using standard linear programming (LP) algorithms. However, the simplicity of the current specification has its own drawback – when several quantiles are estimated, some of the quantile curves may cross each other. In the following subsection the *penalized convex expectile regression* (pCQR) is introduced to solve this drawback.

3.2. Penalized convex quantile regression (pCQR)

To solve the crossing quantile problem Dai et al. (2022) propose the following formulation of penalized convex quantile regression using the L_2 -norm regularization on subgradients $\boldsymbol{\beta}_i$:

$$\begin{aligned}
\min_{\alpha, \boldsymbol{\beta}, \varepsilon^+, \varepsilon^-} \quad & \tau \sum_{i=1}^n \varepsilon_i^+ + (1 - \tau) \sum_{i=1}^n \varepsilon_i^- + \gamma \sum_{i=1}^n \|\boldsymbol{\beta}_i\|_2^2 \\
\text{s.t.} \quad & q_i = \alpha_i + \boldsymbol{\beta}_i^\top \mathbf{k}_i + \varepsilon_i^+ - \varepsilon_i^- & \forall i \\
& \alpha_i + \boldsymbol{\beta}_i^\top \mathbf{k}_i \leq \alpha_s + \boldsymbol{\beta}_s^\top \mathbf{k}_i & \forall i, s, \quad i \neq s \\
& \varepsilon_i^+ \geq 0, \quad \varepsilon_i^- \geq 0 & \forall i
\end{aligned} \tag{10}$$

Here the $\gamma \geq 0$ is the tuning parameter, and $\|\cdot\|_2^2$ is the standard Euclidean norm. With $\gamma \rightarrow 0$ the pCQR problem (10) collapses to the original CQR problem (9).

The pCQR method avoids quantile crossing based on the rationale that as the regularization parameter $\gamma \rightarrow \inf$, the regularization term dominates the minimization process, causing all estimated subgradients $\boldsymbol{\beta}_i$ to converge towards 0. This leads to the estimated quantile functions being represented by horizontal lines (in the 1-dimensional cases) or planes (in the multidimensional cases). It means, that with a large enough γ , the quantile crossing can clearly be avoided. Dai et al. (2022) propose to iteratively find the smallest γ for which no quantile crossing occurs. In practice, the suitable value of γ also depends on the selected quantiles τ to be estimated. Finally, an added advantage of the penalty term is the guaranteed uniqueness of the optimal $(\hat{\alpha}_i, \hat{\boldsymbol{\beta}}_i)$ coefficients.

4. Bagging

The CNLS problem (4) and CQR problem (9) can be solved using the state-of-the-art quadratic programming (QP) and linear programming (LP) solvers, respectively. While these solvers are effective for small datasets (about several hundreds of observations), they are not well-suited to large datasets, such as those commonly encountered in traffic data. For example, data from a 2-lane loop detector for just 10 days of peak hours can contain as many as 3360 observations, which can take a substantial amount of computational time. Furthermore, for the CQR problem on the density-flow plane adding one more observation will increase the number of unknown parameters by 4 and the number of convexity constraints

by $2n$, where n is an overall number of observations. Also, the data on the density-flow plane is skewed: in the free-flow part of the diagram there are numerous observations, that do not bring much insight, compared to a relatively scarce, but important congested part of the diagram.

To facilitate the estimation of the fundamental diagram on arbitrary large datasets, we propose a computational technique referred to as *bagging*. There exist different approaches introduced by, for example, Hannah & Dunson (2013) and Qu et al. (2017), however, we develop a tailored approach for the convex quantile regression.⁵

In practice, *bagging* involves restricting the number of observations to a level at which linear programming solvers can perform efficiently with the minimal loss of precision. This is achieved by aggregating the data on the density-flow plane and dividing it into a set of *bags*, each of which is represented by a centroid describing the data points contained within the bag. The number of bags is determined by dividing the k -axis into u segments and the q -axis into v segments, with the intersection of each u and v segment defining a bag. Each bag contains a set of points $S_j = \{(k_1, q_1), (k_2, q_2), \dots, (k_p, q_p)\}$, $p = |S_j|$, $j \in U \times V$, $U = \{1, \dots, u\}$, $V = \{1, \dots, v\}$, and the centroid, a representative point (k_j^{bag}, q_j^{bag}) for a bag $j \in U \times V$, is calculated as:

$$(k_j^{bag}, q_j^{bag}), k_j^{bag} = \sum_{i=1}^p \frac{k_i}{p}, q_j^{bag} = \sum_{i=1}^p \frac{q_i}{p} \quad (11)$$

As bags may contain varying numbers of observations, it is necessary to account for this discrepancy. To do so, we calculate the weight of each bag based on the number of observations it contains. Specifically, the weight of a bag $w_j = p_j/n$ is calculated as the ratio of the number of observations contained within the bag p_j to the total number of observations n . Therefore, $0 \leq w_j \leq 1 \forall j \in |U \times V|$ and $\sum_{j=1}^{|U \times V|} w_j = 1$.

Figure 2 illustrates an example of the bagging process applied to a dataset of 5-minute yearly observations from a traffic measurement station in Finland over a period of one year,

⁵Hildreth (1954) proposes to aggregate data on the horizontal axis and taking an average of the vertical axis values for an aggregation. While such method gives even more substantial reduction in amount of data points, it is not possible to use it here, as it makes the variation of y -axis non existent, so the quantiles can not be estimated.

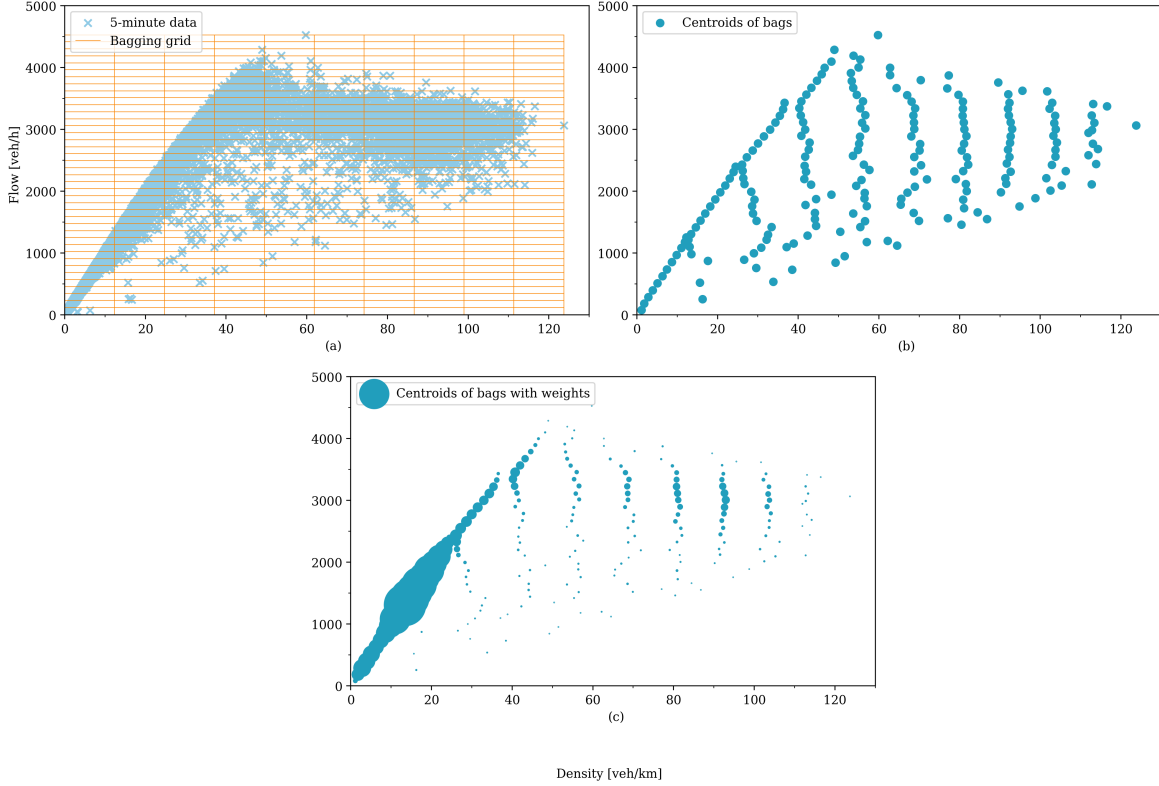


Figure 2: Visualisation of bagging process

comprising 61109 observations. In this example, the bagging grid has a relatively small number of bags ($u = 10$, $v = 40$) for the purpose of demonstrating the approach. As shown in part b) of Figure 2, the application of the bagging process results in a substantial reduction in the number of observations, which are to be represented by the centroids of the bags. However, it is important to note that the quantiles in this case would differ from the original dataset, as centroids do not account for the varying density of observations within the original dataset. To address this issue, the bagging process also assigns weights to the bags, as depicted in the right-side chart, where the size of each dot represents the weight of the corresponding bag. The higher the weight, the larger the size of the dot. This representation shows that the bagging method takes into account the density of the original observations, ensuring that unique or densely congested parts of the dataset are not overlooked.

The CQR problem, that is formulated for the representative points of the bags (11) and accounts for the weights of the bags, is referred to as *convex quantile regression with bags* (CQRb) and has the following mathematical formulation:

$$\begin{aligned}
\min_{\alpha, \beta, \varepsilon^+, \varepsilon^-} \quad & \tau \sum_{j=1}^{|U \times V|} w_j \varepsilon_j^+ + (1 - \tau) \sum_{j=1}^{|U \times V|} w_j \varepsilon_j^- + \sum_{j=1}^{|U \times V|} \|\beta_j\|_2^2 \\
\text{s.t.} \quad & q_j^{bag} = \alpha_j + \beta_j k_j^{bag} + \varepsilon_j^+ - \varepsilon_j^- \quad \forall j \in |U \times V| \\
& \alpha_j + \beta_j k_j^{bag} \leq \alpha_h + \beta_h k_j^{bag} \quad \forall j, h \in |U \times V|, \quad j \neq h \\
& \varepsilon_j^+ \geq 0, \quad \varepsilon_j^- \geq 0 \quad \forall j \in |U \times V|
\end{aligned} \tag{12}$$

In the CQRb problem, the weights w_j are applied to the errors such that the errors of bags with a larger number of observations are given more importance. The estimation is performed using the representative points (k_j^{bag}, q_j^{bag}) for each bag. In comparison to the classic CQR problem (9), the CQRb problem does not have a monotonicity constraint and includes additional constraints on the weights. The jam density can be obtained as $\frac{-\hat{\alpha}_{\max k}^{bag}}{\hat{\beta}_{\max k}^{bag}}$. The solution of problem 12 yields a unique pair of slope and intercept coefficients $(\hat{\alpha}_j, \hat{\beta}_j)$ for each bag j , resulting in the best possible fit. The piece-wise linear function q is constructed using these pairs $(\hat{\alpha}_j, \hat{\beta}_j)$, meaning $\hat{q}_j^{bag} = \hat{\alpha}_j + \hat{\beta}_j k_j^{bag}$. In practice, the number of segments of a piece-wise linear function is substantially smaller than the number of observations. In the estimation of density-flow relation the meaning β_j is the shockwave speed except for β_1 , which denotes the vehicle speed, which is equal to the shockwave speed in the first piece. To satisfy the property, that at zero density there is zero flow the respective point should be added into the dataset for the estimation.

Table 1: Comparison of computational performance of CQR and CQRb

	CQR	CQRb
Data points	3 360	643
Number of constraints	11 292 960	711 492
Time elapsed	2 060 seconds	112 seconds

To evaluate the performance of the CQR method (9) and the CQRb method (12) data from Finnish roads is used (see Section 5 for the description of data) and the pyStoNED package (Dai et al., 2021) with local optimization are employed. The comparison is conducted on 5-minute data for 10 consecutive days, as using a larger number of days results

in insufficient iterations to solve the problem on raw data, leading to termination of the solver. The results of the comparison are presented in Table 1 and show the average performance of the two methods. In order to facilitate the comparison, the function estimated with the CQRb method on the bagged data is extrapolated to the original dataset using a representation theorem adapted from Kuosmanen (2008).

An example of this is shown in Figure 3 where the orange line represents the estimation on the original 5-minute data and the blue dashed line represents the extrapolation of the CQRb estimation from the bagged data to the original data. It can be observed that the estimated functions are almost identical in shape. While both CQR and CQRb are similar in terms of shape, they differ in computational complexity.

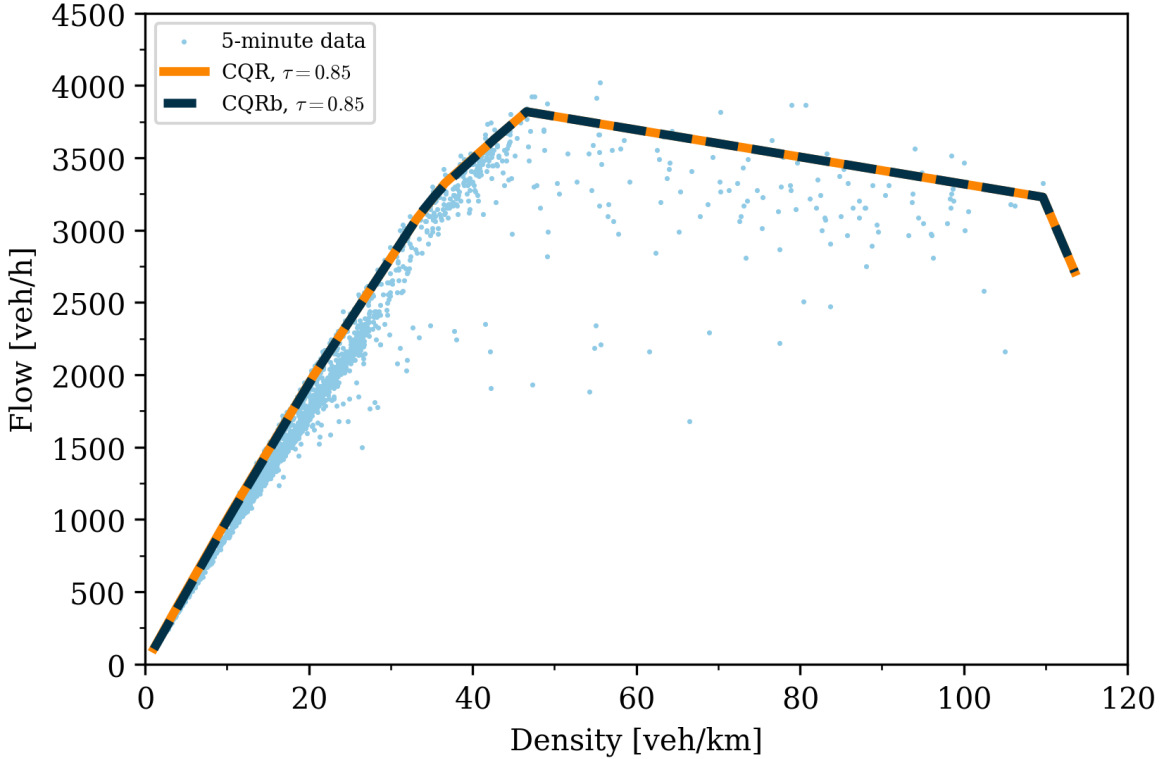


Figure 3: Graphical comparison of estimated function with CQR and CQRb

It is observed that bagging results in a substantially smaller number of data points for CQRb compared to CQR, with the number of data points being more than five times smaller for CQRb. This leads to a reduction in the number of constraints by approximately 16 times. Additionally, the time required for the estimation is reduced from 34 minutes for CQR to

less than 2 minutes for CQRb, including the time for extrapolation from the bagged data to the original 5-minute aggregated data. The results are mentioned for an average run of each method. During the comparison, the parameters u and v for bagging are set to 70 and 400, respectively. While the optimal values of these parameters are subject to further discussion, they are chosen arbitrarily after multiple simulations.

The introduction of CQRb allows to apply CQR for arbitrary large datasets in substantially less time. In the following sections, the CQRb method is applied to data from Finnish roads and compared with the triangular diagram calibration method.

5. Application

For this research, we utilize traffic data provided by Fintraffic / digitraffic.fi (2023) under the Creative Commons 4.0 BY license. There are over 450 traffic measurement stations (TMS) in Finland, but for the purposes of this research, we focus on those located at the busiest road in the Capital region (which includes Helsinki, Espoo, Vantaa, and Kauniainen) and Finland overall, the Ring I (Finnish: Kehä I), numbered Regional Road 101. This 24-kilometer beltway allows vehicles to bypass the center of the capital of Finland, commuting from Espoo and the western districts of Helsinki to the eastern part of Helsinki and back. Figure 4 shows the location of the traffic measurement stations (marked in red) on Ring I (marked blue). Notably, one station is located out of Ring I before the intersection of the Finnish national roads 4 (Lahdenväylä) and 7 (Porvoonväylä) and Ring I, and is of interest due to the high volume of traffic passing through.

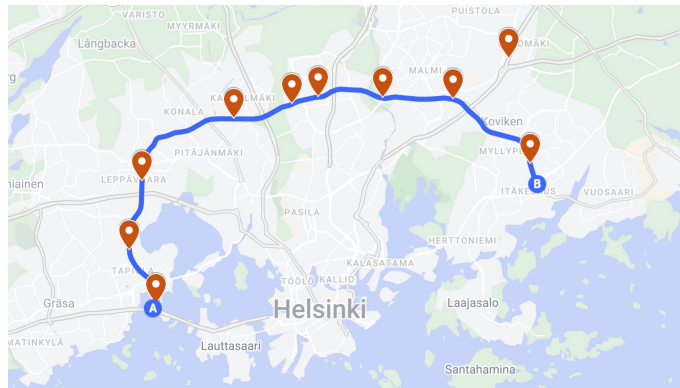


Figure 4: Location of traffic measurement stations around Ring I in Helsinki (Source: Google Maps)

We work with the raw data, which contains information about every vehicle passing the loop detector, to ensure the flexibility in data analysis. In addition the precise time, direction, speed, length and vehicle type are also available. The raw data is aggregated into 5-minute intervals over which harmonic time-average speeds are estimated. These speeds provide a good approximation of the arithmetic space mean speeds. In general, the 5-minute interval is considered to be long enough for fundamental diagram estimation purposes (Wang et al., 2011; Coifman, 2014, 2015; Ponnu & Coifman, 2015; Coifman et al., 2016). The use of 5-minute intervals allows for the assumption of stationary traffic conditions and provides a balance between the variability of 1-minute intervals and the lack of data in 10-minute intervals. The resulting aggregated data is used for estimation purposes.

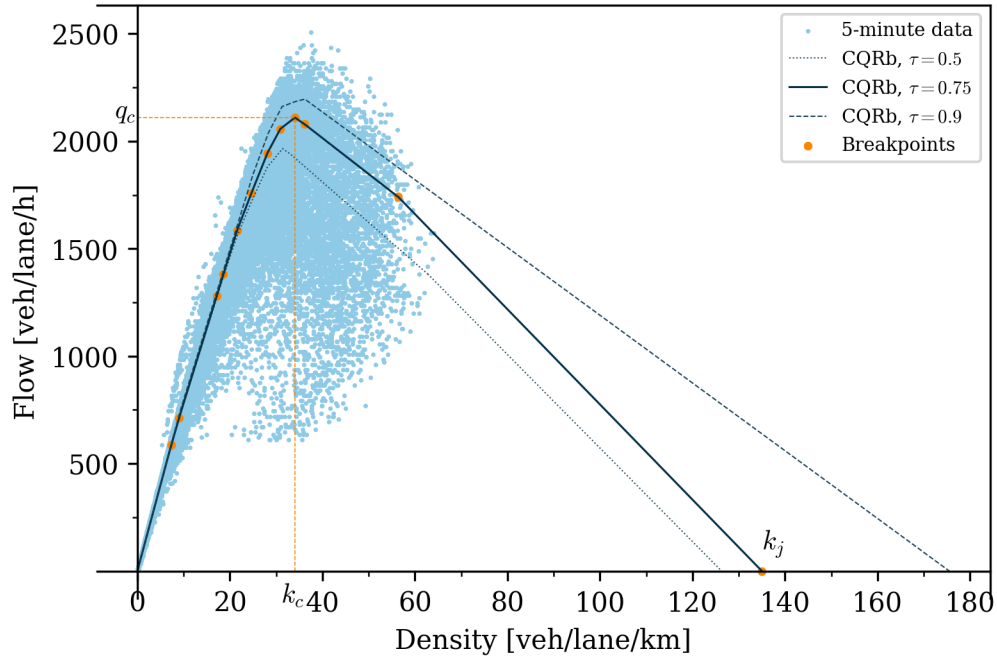


Figure 5: Example of density-flow relations estimation using CQRb

In order to illustrate an example of the CQRb approach, data for TMS 146 for the whole year 2018 is used. The traffic measurement station is located on a road section featuring three eastbound lanes. To account for the specifics of the road traffic in Finland solely peak hours between 6:00 and 20:00 are analyzed. During other periods of time, the traffic volume is low, and congestion does not occur, hence these hours are excluded. The original dataset includes more than 16 million observations, namely vehicles. These are aggregated into 5-

minutes intervals for each lane separately, resulting in a total of 183 465 aggregated data points. Further we apply the bagging procedure with the density-axis divided into 20 equal segments, and the flow-axis divided into 200 equal segments. The final dataset includes 1 614 data points, which are used in the estimation. The number of bags is reduced compared to previous simulations, as it is necessary to keep the number of points within the range of 1 500 – 2 000 to maintain the estimation time at reasonable level.

Figure 5 depicts the CQRb estimation using $\tau = 0.75$ on the aforementioned dataset, as well as $\tau = 0.5$ and $\tau = 0.9$. Following Elefteriadou et al. (2006) we here discuss the $\tau = 0.75$ quantile which describes stable conditions, that are frequently encountered.

The estimation of a piece-wise linear function has formed 12 linear segments, 9 of those located in the free-flow part and 3 in the congested part of the fundamental diagram. It is important to recall that the number of segments is not predetermined, but rather derived solely from the dataset. The equations for each piece are as follows:

$$\hat{q}(k) = \begin{cases} 79.95k & 0 \leq k \leq 7.35 \\ 75.45k + 33.10 & 7.35 \leq k \leq 9.02 \\ 69.79k + 84.14 & 9.02 \leq k \leq 17.13 \\ 69.78k + 84.37 & 17.13 \leq k \leq 18.57 \\ 68.67k + 104.97 & 18.57 \leq k \leq 21.54 \\ 56.11k + 375.51 & 21.54 \leq k \leq 24.63 \\ 53.93k + 429.21 & 24.63 \leq k \leq 28.06 \\ 40.44k + 807.74 & 28.06 \leq k \leq 30.89 \\ 16.61k + 1543.74 & 30.89 \leq k \leq 34.02 \\ -14.03k + 2585.99 & 34.02 \leq k \leq 36.14 \\ -16.71k + 2683.16 & 36.14 \leq k \leq 56.33 \\ -22.14k + 2988.56 & 56.33 \leq k \leq 135.01 \end{cases} \quad (13)$$

The key characteristics of the fundamental diagram are easy to observe. Capacity, which is taken as the maximum flow reached, is $q_c = 2109 \text{ vplph}$ at the critical density of $k_c = 34 \text{ vplpkm}$. The jam density is $k_j = 135 \text{ vplpkm}$, which is obtained as $\frac{-\hat{\alpha}_{\max k}^{bag}}{\hat{\beta}_{\max k}^{bag}}$. It is important to note that despite using an exact number for the capacity, the CQRb method is still regarded as a stochastic capacity approach, as capacity varies depending on the selected quantile. There are 12 different wave speeds, each corresponding to a distinct linear segment

with its own slope representing the shockwave speed. For the free flow part it is necessary to mention the decline of speed with the density growth, and the closer to the critical density, the faster the speed declines, which is depicted by the increasing number of line segments and their lower slope. This phenomenon aligns with the actual road conditions, as more vehicles on the road result in slower speeds and fewer opportunities for lane changes. The speed limit at the observed road section is 80 km/h , and vehicles initially travel at this speed at low densities, slowing down to 70 km/h at the density of 26 vpl/km and flow of 1850 vpl/h . At capacity the speed drops to 62 km/h . The observed reduction in speed is substantial, however, it cannot be captured in the triangular fundamental diagram with the DGKHV calibration approach, as free-flow speed is assumed to be constant across all densities.

In the congested part there are three linear segments with wave speeds of -14.93 , -16.72 and -22.14 . As congestion increases, the shockwave speed also increases in absolute value. The use of several wave speeds provides a more precise description of traffic behavior, demonstrating varying patterns as traffic saturation increases. Although congestion on this road section and in Finland in general is not as severe as in many other countries, the model is still able to capture changes in traffic behavior during congestion periods.

The presented example unveils the efficacy of the CQRb methodology in estimating the density-flow relation of the fundamental diagram. By learning from data, this method provides a more comprehensive representation of the changes in traffic behavior, as evidenced by the multiple linear segments identified in both the free-flow and the congested parts of the diagram. Moreover, since each of the estimated segments in the CQRb method is linear, the resulting wave speeds are readily computed and can be easily incorporated into traffic simulations using the corresponding segment equations. In the next section we will compare the performance of the proposed method with one of the parametric deterministic methods.

6. Out-of-sample performance comparison

In order to conduct the performance comparison, we partition the observed sample to two subsets referred to as the training set and the test set. The training set is a subset of the dataset used to train the predictive model, where it learns patterns and relations between input features and target variables. The test set is a separate subset of the dataset that is

not used during training, but is utilized to evaluate the performance of the model on unseen data. In-sample performance assesses the prediction accuracy of an estimator on the training dataset, while out-of-sample performance evaluates the estimator accuracy on a test dataset (Inoue & Kilian, 2005). The out-of-sample performance provides insight into the ability of the model to predict the future outcomes.

In this section, we aim to compare the performance of the *convex quantile regression with bags* (CQRb) approach with the DGKHV calibration method for a triangular fundamental diagram. To achieve this, we first apply the CQRb approach (12), described in Section 4 to road data from Finland. Next, we apply the DGKHV calibration method introduced by Dervisoglu et al. (2009) to the same data and compare the in-sample and out-of-sample results. Finally, we discuss the proposed CQRb method and present our findings.

The comparison of in-sample and out-of-sample performance incorporates the use of both mean absolute error (MAE, $MAE = \sum_{j=1}^{|U \times V|} |\hat{q}_i^{bag} - q_i^{bag}|$) and root mean squared error (RMSE, $RMSE = \sqrt{\frac{1}{|U \times V|} \sum_{j=1}^{|U \times V|} (\hat{q}_i^{bag} - q_i^{bag})^2}$) as different loss functions are minimized in different methods Geisser (2019) with errors being the lower the better. In terms of loss functions, for the DGKHV approach RMSE is expected to be lower compared to the proposed approach, whereas opposed holds for MAE. For the CQRb approach the MAE is expected to be theoretically lower compared to the DGKHV approach.

To compare the performance between the proposed CQRb method and the DGKHV calibration method for a triangular fundamental diagram, we have collected data from 11 TMS located on Helsinki Ring I and nearby. For TMS located on Ring I both east- and westbound directions are examined, as there are intensive traffic flows in both directions. For the TMS located nearby only the southbound (towards Helsinki) direction is studied, as the intersection is clogged one-way only.

For the aforementioned traffic measurement stations the data has been collected for a period of three years, from 2016 to 2018. In every year data is grouped either by week, either by month periods. While aggregating data within each period into 5-minute time intervals, we consider two different approaches – aggregations by lane or by road direction. Aggregations by lane are aligned with Dervisoglu et al. (2009) and help describe road sections near intersection where the behavior of traffic may vary based on lanes, while aggregations by

road provide a better outlook for TMS located on road sections without nearby intersections. Thereby, there are 4 different aggregations applied to the same data: month-lane, month-road, week-lane, and week-road. Different types of aggregations are necessary to compare behavior between proposed CQRb approach and DGKHV calibration method. However some data might be missing for some days, so there are periods excluded from estimation.

The comparison between the new and the DGKHV approach is conducted through the following procedure. At first, data for one of the 4 aforementioned aggregations is taken for a selected period of time in 2016 or 2017, what forms the training set. Then, using this data, the fundamental diagram is calibrated using both the CQRb method and the DGKHV approach. For the CQRb method three different quantiles are estimated: $\tau \in \{0.75, 0.80, 0.85\}$. This helps us examine the differences between quantiles and account for any external factors that might still affect traffic despite the stationary traffic conditions assumed by the 5-minute intervals. The estimated density-flow relation will reveal the usual operating conditions of the road section. For the DGKHV approach, the scheme proposed in Dervisoglu et al. (2009) is replicated.

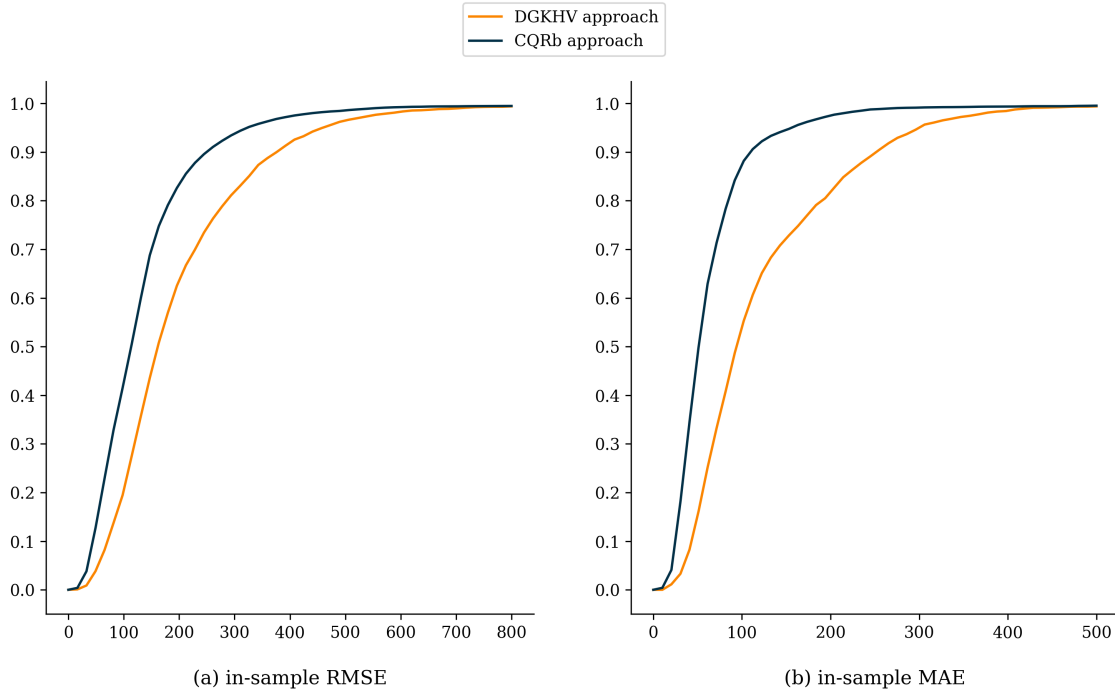


Figure 6: Cumulative distribution for **in-sample** RMSE and MAE

Initially we compare the in-sample performance of two approaches to assess their ability to capture the variation in data. To make this comparison, 11210 test datasets are generated following the principles outlined above. On each dataset we conduct calibration using both CQRb and DGKHV approaches. Notably, the CQRb is estimated on the bagged data and subsequently extrapolated back with the use of the representation theorem to the same aggregated data thereby enabling the computation of errors on identical data. This way the comparison accurately reflects the differences between the two approaches.

Table 2: RMSE and MAE **in-sample** comparison

	RMSE		MAE	
	DGKHV	CQRb	DGKHV	CQRb
week-lane	127.99	99.76	73.19	50.85
week-road	259.54	179.06	168.01	91.30
month-lane	142.57	105.17	80.69	50.42
month-road	298.55	184.19	192.19	83.79
average	199.69	140.60	124.14	70.25

Table 2 provides the averages for four distinct types of aggregations as well as the overall average, with error units measured in *veh/h* for road aggregations and *veh/lane/h* for lane aggregations respectively. Consequently it is expected to have higher errors in road aggregations set side by side with lane aggregations. In terms of performance, CQRb approach exhibits on average 40% improvement in terms of MAE, which is anticipated as the quantile loss function minimizes absolute values. Furthermore, the in-sample RMSE of CQRb approach is smaller by 30% on average, as well as for every type of aggregation, despite the theoretical expectations favouring the DGKHV method. This error comparison provides into how well the estimates capture errors, with the CQRb consistently delivering more precise results, as evidenced by the relative difference within the same type of error. The cumulative distributions of errors presented in Figure 6 indicate that the CQRb approach dominates the DGKHV approach in first-order stochastic terms, which further supports the superiority of the proposed approach.

The subsequent phase entails examining the out-of-sample performance of the estimators, which assesses their ability to predict the density-flow relation one year ahead at the same road section. To account for fluctuating road conditions and traffic seasonality in Finland, we consider comparable time periods for out-of-sample performance. Specifically, for weekly data, we evaluate the same week of the following year compared to the in-sample period, while for monthly data, we assess the same month of the following year relative to the in-sample period, what forms the test set. For instance, if the estimation is done using March 2016 data, we evaluate prediction accuracy on March 2017 data.

Table 3: RMSE and MAE **out-of-sample** comparison

	RMSE OOS		MAE OOS	
	DGKHV	CQRb	DGKHV	CQRb
week-lane	137.17	143.38	77.59	61.77
week-road	288.02	274.91	183.92	128.26
month-lane	150.63	129.75	85.05	58.87
month-road	308.94	227.41	200.52	107.33
average	216.42	202.70	133.46	92.49

Table 3 summarizes the results of out-of-sample predictions errors demonstrating that, CQRb has on average a 6% lower RMSE and 30% lower MAE compared to the DGKHV approach. Notably the RMSE is much closer in comparison to the in-sample results, with the DGKHV approach exhibiting a 5% lower RMSE for the week-lane aggregation, but still higher on average. The cumulative distribution of errors presented in Figure 7 indicates that CQRb dominates the DGKHV approach in second-order stochastic terms, with 92% of RMSE errors and 99% of MAE errors lower than the DGKHV approach.

Analyzing the prediction errors presents an opportunity to assess the predictive power of the proposed approach. Our findings indicate that the CQRb approach demonstrates lower root mean squared errors and mean absolute errors in both in-sample and out-of-sample performances, albeit by a smaller margin in the latter. Consequently, the proposed method is capable of predicting the density-flow relation with greater precision.

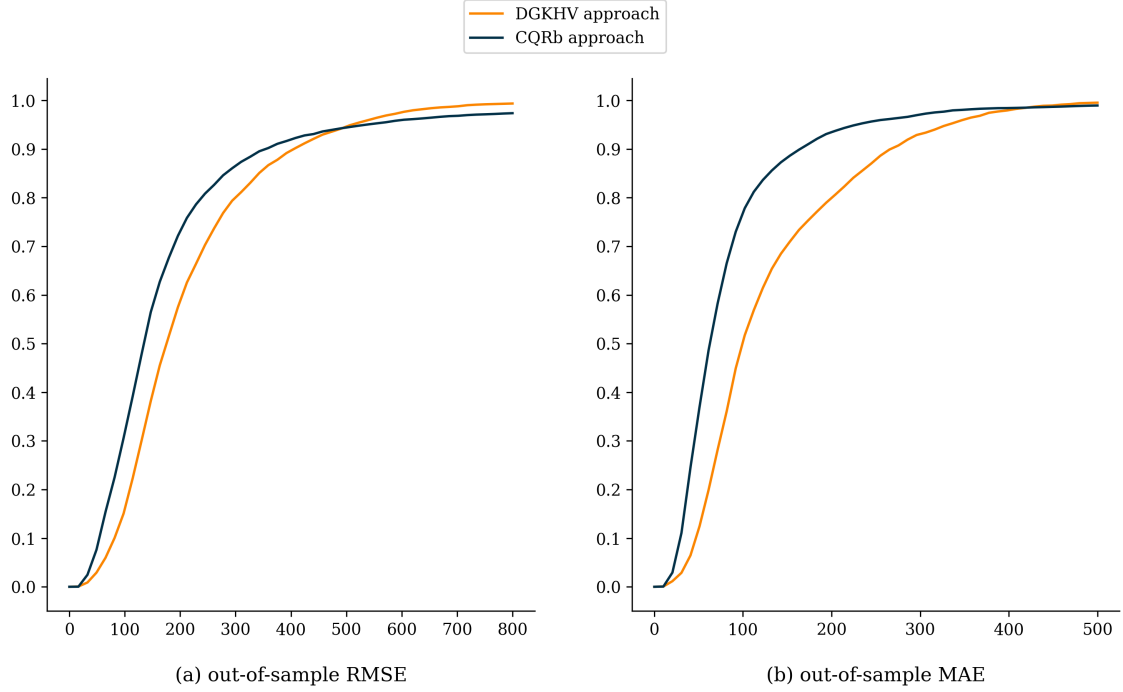


Figure 7: Cumulative distribution for **out-of-sample** RMSE and MAE

The performance comparison highlights the potential of the introduced CQRb method, which consistently achieves lower errors both in-sample and out-of-sample, making it a competitive alternative to the DGKHV calibration method. The CQRb approach provides considerable flexibility in terms of understanding road data and responding to the changes of road state, without the need for deterministic assumptions. Different quantiles τ allow to describe levels of service in different conditions thereby offering a new perspective on traffic flow at a particular road section. With the use of quantiles the stochastic fundamental diagrams are estimated, what is useful for the development and evaluation of control strategies (Jabari & Liu, 2013; Siqueira et al., 2016; Qu et al., 2017). It is widely recognized that the performance of the highway systems can be substantially improved if the heterogeneity of traffic flow dynamics and the stochasticity of the fundamental diagrams can be controlled (Keyvan-Ekbatani et al., 2012; Punzo & Montanino, 2016).

7. Conclusions

In this paper we have introduced a fully nonparametric approach to estimating the stochastic fundamental diagram on the density-flow plane. The method is an extension of the convex quantile regression (CQR) approach and belongs to the convex regression family of models. The piece-wise linear form of the estimated function is capable of representing any arbitrary concave function, making it suitable for estimating the fundamental diagram from empirical data, without having any restrictions on the number or location of pieces imposed. The proposed method satisfies the theoretical properties of the fundamental diagram.

Second, we demonstrate how the methodology can be expressed in the form of a linear programming problem for a general case, and by adapting it for the needs of traffic flow theory research with the adaptation termed *convex quantile regression with bags* (CQRb). A special approach, named bagging, is introduced to account for the computational complexity of the method that arises from the large volume of traffic data necessary for an estimation. This approach substantially decreases the time required for the estimation of a regression function.

The application of the proposed method to the real-world road sensor data from Finland shows how the classic properties of the fundamental diagram are followed with multiple linear segments describing both the free-flow and congested parts of the fundamental diagram offering a better capture of the variance in data. The linear nature of segments allows to determine the shockwave speeds and is preferential for traffic simulation purposes.

Third, the paper demonstrates the predictive power of the CQRb approach through comparisons of the mean absolute error (MAE) and root mean squared error (RMSE) in-sample and out-of-sample performance between CQRb and the DGKHV approach. Consistently lower errors across numerous estimations reveal the potential of the proposed approach and its ability to capture the variance in real-world data.

The proposed approach opens several interesting avenues for future research. For example, it would be worth to investigate how the results obtained from the estimation with the CQRb can be further used for simulation and modeling purposes. We believe that the introduced approach will provide researchers working with mesoscopic and macroscopic models a

more data-driven perspective on the density-flow relation. The approach can be highly beneficial for policy makers, as the new road control strategies can be developed from this more in-depth understanding of density-flow relation. The development of a user-friendly tool, which would allow researchers and practitioners to apply the proposed method, is underway as the authors currently adapt their developments for the third-party use.

Acknowledgements

The authors acknowledge the computational resources provided by the Aalto Science-IT project. Iaroslav Kriuchkov gratefully acknowledges financial support from Liikesivistysrahasto (210036) and KAUTE-säätiö (20220231).

References

- Ansorge, R. (1990). What does the entropy condition mean in traffic flow theory? *Transportation Research Part B: Methodological*, 24, 133–143. doi:10.1016/0191-2615(90)90024-S.
- Bigazzi, A. Y., & Figliozzi, M. A. (2013). Marginal costs of freeway traffic congestion with on-road pollution exposure externality. *Transportation Research Part A: Policy and Practice*, 57, 12–24. doi:10.1016/j.tra.2013.09.008.
- Bramich, D. M., Menéndez, M., & Ambühl, L. (2022). Fitting Empirical Fundamental Diagrams of Road Traffic: A Comprehensive Review and Comparison of Models Using an Extensive Data Set. *IEEE Transactions on Intelligent Transportation Systems*, 23, 14104–14127. doi:10.1109/TITS.2022.3142255.
- Cassidy, M. J., & Bertini, R. L. (1999). Some traffic features at freeway bottlenecks. *Transportation Research Part B: Methodological*, 33, 25–42. doi:10.1016/S0191-2615(98)00023-X.
- del Castillo, J. M. (2012). Three new models for the flow–density relationship: derivation and testing for freeway and urban data. *Transportmetrica*, 8, 443–465. doi:10.1080/18128602.2011.556680.

- Castillo, J. M. D., & Benitez, F. G. (1995). On the functional form of the speed-density relationship—I: General theory. *Transportation Research Part B: Methodological*, 29, 373–389. doi:10.1016/0191-2615(95)00008-2.
- Chanut, S., & Buisson, C. (2003). Macroscopic Model and Its Numerical Solution for Two-Flow Mixed Traffic with Different Speeds and Lengths. *Transportation Research Record*, 1852, 209–219. doi:10.3141/1852-26.
- Chen, X. (2007). Large Sample Sieve Estimation of Semi-Nonparametric Models. In J. J. Heckman, & E. E. Leamer (Eds.), *Handbook of Econometrics* (pp. 5549–5632). volume 6B.
- Coifman, B. (2014). Revisiting the empirical fundamental relationship. *Transportation Research Part B: Methodological*, 68, 173–184. doi:10.1016/j.trb.2014.06.005.
- Coifman, B. (2015). Empirical flow-density and speed-spacing relationships: Evidence of vehicle length dependency. *Transportation Research Part B: Methodological*, 78, 54–65. doi:10.1016/j.trb.2015.04.006.
- Coifman, B., Wu, M., Redmill, K., & Thornton, D. A. (2016). Collecting ambient vehicle trajectories from an instrumented probe vehicle: High quality data for microscopic traffic flow studies. *Transportation Research Part C: Emerging Technologies*, 72, 254–271. doi:10.1016/j.trc.2016.09.001.
- Daganzo, C. F. (1994). The cell transmission model: A dynamic representation of highway traffic consistent with the hydrodynamic theory. *Transportation Research Part B: Methodological*, 28, 269–287. doi:10.1016/0191-2615(94)90002-7.
- Daganzo, C. F. (2005). A variational formulation of kinematic waves: basic theory and complex boundary conditions. *Transportation Research Part B: Methodological*, 39, 187–196. doi:10.1016/j.trb.2004.04.003.
- Daganzo, C. F., Cassidy, M. J., & Bertini, R. L. (1999). Possible explanations of phase transitions in highway traffic. *Transportation Research Part A: Policy and Practice*, 33, 365–379. doi:10.1016/S0965-8564(98)00034-2.

- Daganzo, C. F., & Geroliminis, N. (2008). An analytical approximation for the macroscopic fundamental diagram of urban traffic. *Transportation Research Part B: Methodological*, 42, 771–781. doi:10.1016/j.trb.2008.06.008.
- Dai, S., Fang, Y.-H., Lee, C.-Y., & Kuosmanen, T. (2021). pyStoNED: A Python Package for Convex Regression and Frontier Estimation. doi:10.48550/arXiv.2109.12962.
- Dai, S., Kuosmanen, T., & Zhou, X. (2022). Non-crossing convex quantile regression. doi:10.48550/arXiv.2204.01371.
- Dai, S., Kuosmanen, T., & Zhou, X. (2023). Generalized quantile and expectile properties for shape constrained nonparametric estimation. *European Journal of Operational Research*, 310, 914–927. doi:10.1016/j.ejor.2023.04.004.
- Dervisoglu, G., Gomes, G., Kwon, J., Horowitz, R., & Varaiya, P. P. (2009). Automatic Calibration of the Fundamental Diagram and Empirical Observations on Capacity. In *Transportation Research Board 88th Annual Meeting*. Washington DC, United States.
- Edie, L. C. (1961). Car-Following and Steady-State Theory for Noncongested Traffic. *Operations Research*, 9, 66–76. doi:10.1287/opre.9.1.66.
- Elefteriadou, L., Hall, F. L., Brilon, W., Roess, R. P., & Romana, M. G. (2006). Revisiting the Definition and Measurement of Capacity. In *Revisiting the definition and measurement of capacity*.
- Fan, S., & Seibold, B. (2013). Data-Fitted First-Order Traffic Models and Their Second-Order Generalizations: Comparison by Trajectory and Sensor Data. *Transportation Research Record*, 2391, 32–43. doi:10.3141/2391-04.
- Figliozi, M. A. (2011). The impacts of congestion on time-definitive urban freight distribution networks CO2 emission levels: Results from a case study in Portland, Oregon. *Transportation Research Part C: Emerging Technologies*, 19, 766–778. doi:10.1016/j.trc.2010.11.002.

- Fintraffic / digitraffic.fi (2023). Information about open data for application development from Finnish road, railway and marine traffic. URL: <https://www.digitraffic.fi/en/>.
- Geisser, S. (2019). *Predictive Inference*. New York: Chapman and Hall/CRC. doi:10.1201/9780203742310.
- Gipps, P. G. (1981). A behavioural car-following model for computer simulation. *Transportation Research Part B: Methodological*, 15, 105–111. doi:10.1016/0191-2615(81)90037-0.
- Greenshields, B., Bibbins, J., Channing, W., & Miller, H. (1935). A study of traffic capacity. *Proceedings of the 14th Annual Meeting of the Highway Research Board*, 1935.
- Guériau, M., Billot, R., El Faouzi, N.-E., Monteil, J., Armetta, F., & Hassas, S. (2016). How to assess the benefits of connected vehicles? A simulation framework for the design of cooperative traffic management strategies. *Transportation Research Part C: Emerging Technologies*, 67, 266–279. doi:10.1016/j.trc.2016.01.020.
- Hall, F. L., & Agyemang-Duah, K. (1991). Freeway Capacity Drop and the Definition of Capacity. *Transportation Research Record*, (pp. 91–98).
- Hannah, L. A., & Dunson, D. B. (2013). Multivariate Convex Regression with Adaptive Partitioning. *Journal of Machine Learning Research*, 14, 3261–3294.
- Hanson, D. L., & Pledger, G. (1976). Consistency in Concave Regression. *The Annals of Statistics*, 4, 1038–1050.
- Hernandez, J. Z., Ossowski, S., & Garcia-Serrano, A. (2002). Multiagent architectures for intelligent traffic management systems. *Transportation Research Part C: Emerging Technologies*, 10, 473–506. doi:10.1016/S0968-090X(02)00032-3.
- Hildreth, C. (1954). Point Estimates of Ordinates of Concave Functions. *Journal of the American Statistical Association*, 49, 598–619. doi:10.1080/01621459.1954.10483523.
- Hoogendoorn, S. P., & Bovy, P. H. L. (1998). New Estimation Technique for Vehicle-Type-Specific Headway Distributions. *Transportation Research Record*, 1646, 18–28. doi:10.3141/1646-03.

- Inoue, A., & Kilian, L. (2005). In-Sample or Out-of-Sample Tests of Predictability: Which One Should We Use? *Econometric Reviews*, 23, 371–402. doi:10.1081/ETC-200040785.
- Jabari, S. E., & Liu, H. X. (2012). A stochastic model of traffic flow: Theoretical foundations. *Transportation Research Part B: Methodological*, 46, 156–174. doi:10.1016/j.trb.2011.09.006.
- Jabari, S. E., & Liu, H. X. (2013). A stochastic model of traffic flow: Gaussian approximation and estimation. *Transportation Research Part B: Methodological*, 47, 15–41. doi:10.1016/j.trb.2012.09.004.
- Kerner, B. S. (2009). *Introduction to Modern Traffic Flow Theory and Control: The Long Road to Three-Phase Traffic Theory*. Berlin, Heidelberg: Springer. doi:10.1007/978-3-642-02605-8.
- Kerner, B. S., & Konhäuser, P. (1994). Structure and parameters of clusters in traffic flow. *Physical Review E*, 50, 54–83. doi:10.1103/PhysRevE.50.54.
- Keyvan-Ekbatani, M., Kouvelas, A., Papamichail, I., & Papageorgiou, M. (2012). Exploiting the fundamental diagram of urban networks for feedback-based gating. *Transportation Research Part B: Methodological*, 46, 1393–1403. doi:10.1016/j.trb.2012.06.008.
- Koenker, R. (2005). *Quantile Regression*. Econometric Society Monographs. Cambridge: Cambridge University Press. doi:10.1017/CB09780511754098.
- Koenker, R., & Bassett, G. (1978). Regression Quantiles. *Econometrica*, 46, 33–50. doi:10.2307/1913643.
- Koshi, M., Iwasaki, M., & Ohkura, I. (1983). Some Findings and an Overview on Vehicular Flow Characteristics. In V. F. Hurdle, E. Hauer, & G. N. Steuart (Eds.), *Proceedings of the Eighth International Symposium on Transportation and Traffic Theory* (pp. 403–426).
- Kuosmanen, T. (2008). Representation theorem for convex nonparametric least squares. *The Econometrics Journal*, 11, 308–325. doi:10.1111/j.1368-423X.2008.00239.x.

- Kuosmanen, T., Johnson, A., & Saastamoinen, A. (2015). Stochastic Nonparametric Approach to Efficiency Analysis: A Unified Framework. In J. Zhu (Ed.), *Data Envelopment Analysis: A Handbook of Models and Methods* International Series in Operations Research & Management Science (pp. 191–244). Boston, MA: Springer US. doi:10.1007/978-1-4899-7553-9_7.
- Kuosmanen, T., & Johnson, A. L. (2010). Data Envelopment Analysis as Nonparametric Least-Squares Regression. *Operations Research*, 58, 149–160. doi:10.1287/opre.1090.0722.
- Lee, C.-Y., Johnson, A. L., Moreno-Centeno, E., & Kuosmanen, T. (2013). A more efficient algorithm for Convex Nonparametric Least Squares. *European Journal of Operational Research*, 227, 391–400. doi:10.1016/j.ejor.2012.11.054.
- Li, J., & Zhang, H. M. (2011). Fundamental Diagram of Traffic Flow: New Identification Scheme and Further Evidence from Empirical Data. *Transportation Research Record*, 2260, 50–59. doi:10.3141/2260-06.
- Lighthill, M. J., & Whitham, G. B. (1955). On kinematic waves II. A theory of traffic flow on long crowded roads. *Proceedings of the Royal Society of London. Series A. Mathematical and Physical Sciences*, 229, 317–345. doi:10.1098/rspa.1955.0089.
- Muralidharan, A., Dervisoglu, G., & Horowitz, R. (2011). Probabilistic Graphical Models of Fundamental Diagram Parameters for Simulations of Freeway Traffic. *Transportation Research Record*, 2249, 78–85. doi:10.3141/2249-10.
- Newell, G. F. (1993). A simplified theory of kinematic waves in highway traffic, part I: General theory. *Transportation Research Part B: Methodological*, 27, 281–287. doi:10.1016/0191-2615(93)90038-C.
- Ponnu, B., & Coifman, B. (2015). Speed-spacing dependency on relative speed from the adjacent lane: New insights for car following models. *Transportation Research Part B: Methodological*, 82, 74–90. doi:10.1016/j.trb.2015.09.012.

- Punzo, V., & Montanino, M. (2016). Speed or spacing? Cumulative variables, and convolution of model errors and time in traffic flow models validation and calibration. *Transportation Research Part B: Methodological*, *91*, 21–33. doi:10.1016/j.trb.2016.04.012.
- Qu, X., Wang, S., & Zhang, J. (2015). On the fundamental diagram for freeway traffic: A novel calibration approach for single-regime models. *Transportation Research Part B: Methodological*, *73*, 91–102. doi:10.1016/j.trb.2015.01.001.
- Qu, X., Zhang, J., & Wang, S. (2017). On the stochastic fundamental diagram for freeway traffic: Model development, analytical properties, validation, and extensive applications. *Transportation Research Part B: Methodological*, *104*, 256–271. doi:10.1016/j.trb.2017.07.003.
- Richards, P. I. (1956). Shock Waves on the Highway. *Operations Research*, *4*, 42–51.
- Roncoli, C., Bekiaris-Liberis, N., & Papageorgiou, M. (2016). Optimal lane-changing control at motorway bottlenecks. In *2016 IEEE 19th International Conference on Intelligent Transportation Systems (ITSC)* (pp. 1785–1791). doi:10.1109/ITSC.2016.7795800.
- Shaygan, M., Meese, C., Li, W., Zhao, X. G., & Nejad, M. (2022). Traffic prediction using artificial intelligence: Review of recent advances and emerging opportunities. *Transportation Research Part C: Emerging Technologies*, *145*, 103921. doi:10.1016/j.trc.2022.103921.
- Siqueira, A. F., Peixoto, C. J. T., Wu, C., & Qian, W.-L. (2016). Effect of stochastic transition in the fundamental diagram of traffic flow. *Transportation Research Part B: Methodological*, *87*, 1–13. doi:10.1016/j.trb.2016.02.003.
- Smulders, S. (1990). Control of freeway traffic flow by variable speed signs. *Transportation Research Part B: Methodological*, *24*, 111–132. doi:10.1016/0191-2615(90)90023-R.
- Tadaki, S.-i., Kikuchi, M., Fukui, M., Nakayama, A., Nishinari, K., Shibata, A., Sugiyama, Y., Yosida, T., & Yukawa, S. (2015). Critical Density of Experimental Traffic Jam. In M. Chraïbi, M. Boltes, A. Schadschneider, & A. Seyfried (Eds.), *Traffic and Granular Flow '13* (pp. 505–511). Cham: Springer International Publishing. doi:10.1007/978-3-319-10629-8_56.

- Treiber, M., Kesting, A., & Helbing, D. (2006). Understanding widely scattered traffic flows, the capacity drop, and platoons as effects of variance-driven time gaps. *Physical Review E*, *74*, 016123. doi:10.1103/PhysRevE.74.016123.
- Wang, H., Li, J., Chen, Q.-Y., & Ni, D. (2011). Logistic modeling of the equilibrium speed–density relationship. *Transportation Research Part A: Policy and Practice*, *45*, 554–566. doi:10.1016/j.tra.2011.03.010.
- Wang, H., Ni, D., Chen, Q.-Y., & Li, J. (2013). Stochastic modeling of the equilibrium speed–density relationship. *Journal of Advanced Transportation*, *47*, 126–150. doi:10.1002/atr.172.
- Wang, S., Chen, X., & Qu, X. (2021). Model on empirically calibrating stochastic traffic flow fundamental diagram. *Communications in Transportation Research*, *1*, 100015. doi:10.1016/j.commtr.2021.100015.
- Wang, Y., Wang, S., Dang, C., & Ge, W. (2014). Nonparametric quantile frontier estimation under shape restriction. *European Journal of Operational Research*, *232*, 671–678. doi:10.1016/j.ejor.2013.06.049.
- Wu, N. (2002). A new approach for modeling of Fundamental Diagrams. *Transportation Research Part A: Policy and Practice*, *36*, 867–884. doi:10.1016/S0965-8564(01)00043-X.
- Yagi, D., Chen, Y., Johnson, A. L., & Kuosmanen, T. (2020). Shape-Constrained Kernel-Weighted Least Squares: Estimating Production Functions for Chilean Manufacturing Industries. *Journal of Business & Economic Statistics*, *38*, 43–54. doi:10.1080/07350015.2018.1431128.
- Zhang, H. M. (1999). A mathematical theory of traffic hysteresis. *Transportation Research Part B: Methodological*, *33*, 1–23. doi:10.1016/S0191-2615(98)00022-8.